PHYSICAL REVIEW B **78**, 035328 (2008)

Thickness-tunable terahertz plasma oscillations in a semiconductor slab excited by femtosecond optical pulses

Y. D. Glinka,* D. Maryenko, and J. H. Smet

Max-Planck-Institut fur Festkörperforschung, Heisenberg Str. 1, 70569 Stuttgart, Germany

(Received 9 March 2008; revised manuscript received 1 May 2008; published 24 July 2008)

We report on the observation of terahertz oscillations in an electron-hole plasma optically excited by a femtosecond pulse in the μm-sized slab of low-temperature-grown-GaAs (LT-GaAs) grown on the GaAs substrate. The frequency of oscillations is shown to be inversely proportional to the slab thickness. It is suggested that the LT-GaAs slab serves as a resonant cavity for traveling plasma waves, which have been generated as a consequence of the shock interaction of photoexcited electron plasma with the GaAs/LT-GaAs interface. The instantaneous diffusion of photoexcited plasma inward the material is driven by the density gradient over the Beer's law distributed carrier population and is evidenced to be a main reason of the shock interaction in the localized plasma. The frequencies of oscillations observed are 3.5 times larger that the inverse electron transit time in the LT-GaAs slab, suggesting the "ballistic" regime for plasma wave propagation to occur. The oscillations have been observed in the photocurrent autocorrelation measurements. The dynamical electric field at the GaAs/LT-GaAs interface arising due to the instantaneous diffusion of photoexcited electrons inward the material was studied through the transient reflectivity change responses, which have been measured simultaneously with photocurrent.

DOI: 10.1103/PhysRevB.78.035328 PACS number(s): 68.49.−h, 42.79.Ta, 52.35.−g, 82.53.Mj

I. INTRODUCTION

Terahertz (THz) oscillations generated in semiconductors by an ultrashort light pulse is known to be due to coherent effects in the photogenerated plasma during optical excitation in the surface depletion region or in the electric field region of a biased semiconductor.[1,2] The effect is normally explained as a screening of the build-in or applied surface field by the photogenerated carriers. Accordingly, the initial acceleration of photoexcited electrons and holes in the surface field region induces a polarization, which acts as the restoring force of the carrier motion. The resulting plasma oscillations with the frequency $\omega=\sqrt{\omega_p-\gamma^2/4}$ are determined by the damping rate γ and the plasma frequency $\omega_p=\sqrt{n_q q^2/\varepsilon\varepsilon_0 m^*}$, where n_q is the density of coherently oscillating carriers, q is the electron charge, m^* is the reduced effective mass, ε is the static permittivity, and ε_0 is the electric constant.[2] As this takes place, the frequency of the few-cycle plasma oscillations can be tuned in the range of 1–10 THz by the density of photoexcited carriers.[1,2] The coherent longitudinal optical (LO) phonon and coupled plasmon-LO-phonon modes with frequencies in the range of 4–9 THz can also be driven resonantly by the initial instantaneous polarization of the photogenerated plasma in the field region.[3–5] Another mechanism for generating THz oscillations takes into account the carrier drift and ballistic transport in the field region and points to the transport-dominated behavior instead of the displacement-dominated one for coherent plasma effects.[6,7] Also, the electron plasma created in semiconductors can spontaneously be broken up into high-frequency oscillations as a consequence of the negative differential resistance (the Gunn effect).[8] The frequency of oscillations in the Gunn effect is inversely proportional to the length of the semiconductor across which the field is applied. Hence, the frequency can be tuned by the sample length and is only limited by the carrier drift saturation velocity.[8] Despite the fact that the frequency of oscillations in the Gunn effect is at least one order of magnitude less than that of plasma oscillations, the frequency range can be extended up to 1.2 THz range by using the frequency multipliers.[9]

An essentially different origin for generating THz oscillations in semiconductors is related to the plasma waves.[10–12] Since the plasma wave frequency is much larger than the inverse electron transit time in the material, it is easier to reach "ballistic" regimes for plasma waves than for electrons moving with drift velocities. Because in the ballistic regime no collisions of electrons with impurities or lattice vibrations occur on a time scale of the order of the plasma oscillation period, the thin slab semiconductors act as a resonant cavity for plasma waves. The key circumstance leading to the plasma wave generation is the bulk plasma instability (Dyakonov–Shur instability) in the semiconductor slab (transistor channel) due to the boundary conditions.[10–12] The fundamental frequency of the resonant cavity can be tuned by changing either the gate bias or the slab thickness (device length). This makes possible tunable resonant detection or emission of the electromagnetic radiation in the THz range in the channel of high electron mobility transistors (HEMT).[10–12] Despite the fact that the prediction for resonant THz emission from the channel of GaAs-based HEMT due to the Dyakonov–Shur instability has been made in 1993, the first observation of voltage tunable resonant THz emission in the range of ~0.4–1.0 THz by plasma generation in a 60 nm InGaAs HEMT has been reported as late as 2004.[13] One of the main experimental difficulties was to achieve the resonant cavity boundary conditions required for the development of plasma instability upon successive reflections of plasma waves from the HEMT channel borders.[12] However, up to now the possibility of the device length for tuning the frequency of resonant THz oscillations in GaAs-based HEMT has not been demonstrated yet.

1098-0121/2008/78(3)/035328(10) ©2008 The American Physical Society

In the current paper we report on THz oscillations in the electron-hole plasma generated by an ultrashort laser pulse in the μm-sized slab of low-temperature-grown-GaAs (LT-GaAs) grown on the GaAs substrate (GaAs/LT-GaAs), which is implemented as a photoconductive switch (PS). We show that the frequency of oscillations that appeared in the photocurrent autocorrelation signals is inversely proportional to the thickness of the LT-GaAs slab. Using the laser photon energy just 20 meV higher than the bandgap of GaAs (E_g $=1.43$ eV) in order to minimize the electron-LO-phonon scattering (LO phonon energy ~36 meV), we observed THz oscillations, the frequency of which is 3.5 times larger than the inverse electron transit time in the LT-GaAs slab. As a result, the "ballistic" regime for plasma wave propagation has been suggested. THz oscillations in the electron plasma manifest themselves in the photocurrent autocorrelation responses as a consequence of the standing plasma waves created in the resonant cavity upon successive reflection of traveling plasma waves from the LT-GaAs slab boundaries. Because the frequency of standing plasma waves generated is much less than ω_p, the microscopic picture of THz oscillations observed can be imagined as a modulation of high-frequency plasma oscillations by the lower frequency plasma wave. The resulting spatial modulation of the photoexcited plasma is the primary source for THz oscillations to appear in the photocurrent autocorrelation signals. The frequency of THz oscillations hence does not depend on the carrier density and is exclusively determined by the resonant cavity width (the thickness of the LT-GaAs slab). As a result, the frequency of oscillations in the THz range can be tuned by the LT-GaAs slab thickness. Based on the transient reflectivity change (TRC) responses, which have been measured simultaneously with photocurrent autocorrelation signals, we recognized that the plasma waves are generated due to the shock interaction of photoexcited electron plasma with the GaAs/LT-GaAs interface. The instantaneous diffusion of photoexcited plasma inward the material is driven by the density gradient over the Beer's law distributed carrier population and is evidenced to be a main reason of the shock interaction in the localized plasma. The THz oscillations due to the plasma wave generation are hence caused by the localization of the photoexcited electron-hole plasma in the LT-GaAs slab. Also, we show that the damping of plasma waves is mainly governed by the trapping of electrons by As cluster point defects in LT-GaAs.

II. EXPERIMENTAL DETAILS

Our experiments were performed with a fast-scan pump-probe setup allowing the photocurrent autocorrelation and TRC responses to be measured simultaneously [Fig. 1(a)]. Two GaAs/LT-GaAs samples of different thicknesses of the LT-GaAs slab (1 and 2 μm) were grown by molecular beam epitaxy on (100)-oriented semi-insulating GaAs substrate at 150 °C. The PS's have been formed by patterning a 3 μm broad gap in the central conductor of a coplanar Au waveguide [Fig. 2(b)]. The initial beam of a mode-locked Ti:Sa laser producing 150-fs pulses with a central photon energy of 1.45 eV or 1.60 eV, a band width of 17 meV, and a repetition rate of 76 MHz was split into two beams, which were set up to be cross polarized and focused with a 100× objective to the spot just covering the PS gap. The orientation of the electric fields of the normally incident collinear laser beams with respect to the applied bias field was set up to 45° [Fig. 1(b)]. The photocurrent has been detected with a transimpedance amplifier and recorded with a sampling oscilloscope as a function of the time delay, which was periodically varied at a frequency of 16 Hz by a shaker scanner. The photocurrent autocorrelation signals obtained were averaged over 1000 delay cycles. The reflected beams from the PS gap were extracted by a splitter [Fig. 1(a)]. One of the beams (hereafter referred to as a probe beam) has been separated from another one (a pump beam) by a polarizer and detected by a photodiode similarly to the electrical responses.

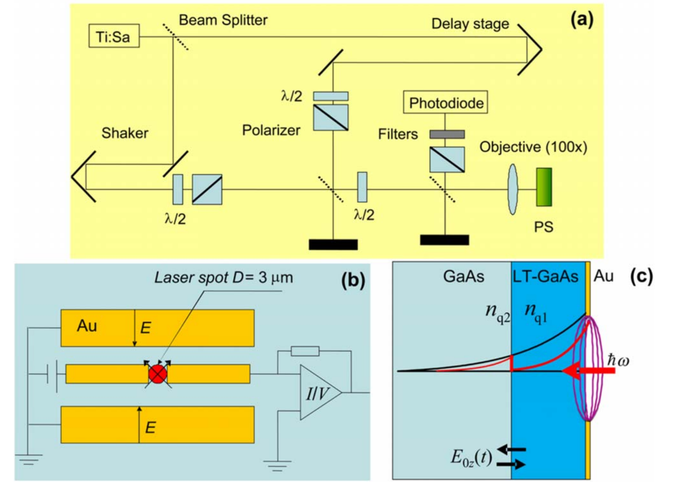

FIG. 1. (Color online) (a) A sketch of the experimental setup used. (b) A schematic top view of the PS and the orientation of the applied and laser beam electric fields. (c) A sketch of the depth section of the PS and the Beer's law electron density distribution due to the laser pulse action (shown in black) and some time after it when electrons in LT-GaAs get partially relaxed (shown in red). The applied electric field lines on the surface are shown schematically.

III. EXPERIMENTAL RESULTS AND DISCUSSION

A. Photocurrent autocorrelation signals and plasma waves generation in the photoexcited plasma localized in the low-temperature-grown-GaAs slab

Figure 2 shows the photocurrent responses from GaAs/LT-GaAs PS's measured in the photocurrent autocorrelation regime,[14,15] at which the laser power of both beams has been set up to be equal. The insets of Fig. 2 show the corresponding TRC responses measured simultaneously with photocurrent signals. First it should be noted that the applied bias field does not affect the TRC signals measured even for the strongest field used (a bias voltage of $U=10$ V). This fact is an indication that the measured optical and electrical signals originate from the different sources. Since the applied bias creates a surface electric field (along the surface, x axis), the photocurrent response is mainly affected by the spatial distribution of photoexcited carriers in the vicinity of the sur-

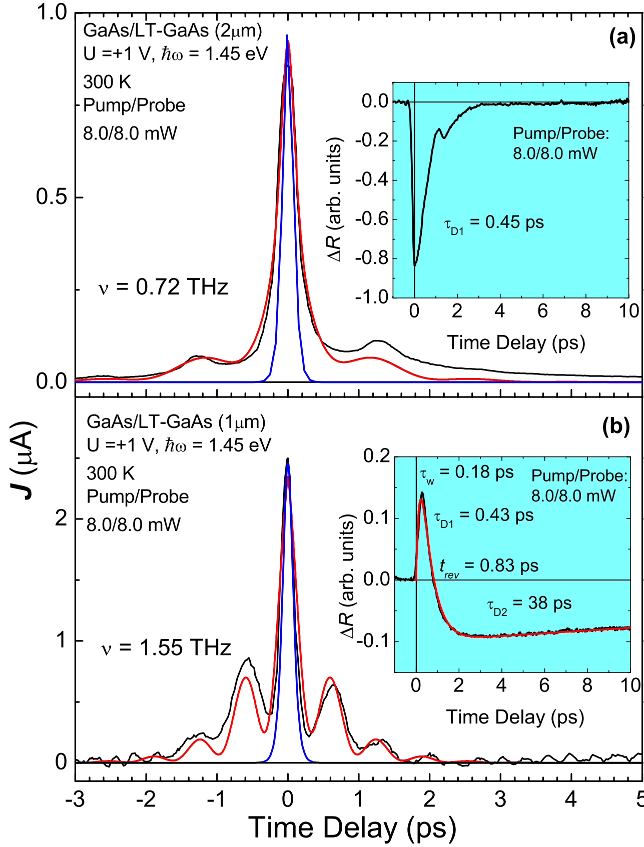

FIG. 2. (Color online) The photocurrent autocorrelation signals from the GaAs/LT-GaAs PS's of different thicknesses of the LT-GaAs slab [2 μm (a) and 1 μm (b)] (black curves) measured under experimental conditions indicated. The results of the fit by Eq. (6) are shown in red. The laser light autocorrelated pulse is presented as a function $\mathrm{sech}^2(1.54^* t/0.15\ \mathrm{ps})$ (blue curves). The insets show the corresponding TRC signals measured simultaneously with photocurrent autocorrelation signals (black curves). The inset of (b) also shows in red the result of the fit by Eq. (10).

face [Fig. 1(c)]. Here we assume that the photoexcited electrons mainly contribute to the ultrafast photocurrent responses since the mobility of electrons in GaAs is known to be much higher than that of holes. Notice that PS's used have a gap of 3 μm, comparable to the depth of the LT-GaAs slab. The field from the bias on these PS's is expected to easily be fringing and having significant z components (perpendicular to the surface and directed inward the material) over the active area of PS's.

Taking into account that the absorption coefficient of GaAs for 1.45-eV light is $\sim 0.9\times 10^4\ \mathrm{cm}^{-1}$, the absorption length according to Beer's law is estimated as $L=1.1\ \mu\mathrm{m}$. As a result, at normal light incidence 60% of the incident light is absorbed in the 1-μm thick LT-GaAs slab while the GaAs substrate absorbs 40% of the light. For the 2-μm thick LT-GaAs slab PS the percentage of the incident light absorbed is 84% and 16%, respectively. This estimation shows that the photoexcited Beer's law distributed carrier population is spatially extended over the GaAs/LT-GaAs interface. This circumstance is considered as a main reason for the generation of plasma waves in the LT-GaAs slab, which appear as THz oscillations in the photocurrent autocorrelation measurements. For the same reason the dynamical electric field at the GaAs/LT-GaAs interface is formed as a consequence of the limited diffusion of photoexcited carriers across the interface. As it will be discussed below, the dynamical electric field contributes into the TRC signals through the electro-optic effect being a dominant local source of the TRC signals at high electron densities excited. The contribution into the TRC signals from the spatially distributed electron population (the absorption bleaching effect) becomes weaker at such densities than the electro-optic contribution. Thus, because of the local character of the dynamical electric field and because the bias field is expected to be extended inward the material for distances much less than the thickness of the LT-GaAs slab, the applied bias field does not affect the TRC signals. Nevertheless, the TRC signals measured simultaneously with photocurrent responses provide unique information about the electric field dynamics at the GaAs/LT-GaAs interface, which plays a primary role in the generation of THz plasma oscillations discussed.

The photocurrent responses shown in Fig. 2 reveal pronounced oscillations in the THz range, the frequency of which is close to be inversely proportional to the thickness of the LT-GaAs slab. As this takes place, the amplitude of oscillations decreases for the thicker slab PS's. The slight asymmetry of the signals results from the imperfect alignment of collinear laser beams used with respect to each other and to the PS gap. It is interesting that the corresponding TRC signals do not reveal any oscillations. We will show below that this is caused by the peculiarity of plasma standing-wave formation within the LT-GaAs slab. The Fourier transformation of the oscillatory part of the signals gives the frequencies of 1.55 and 0.72 THz for the samples of 1-μm and 2-μm thick LT-GaAs slab, respectively (Figs. 2 and 3). The frequencies of oscillations are out of the range of the coherent LO phonon and coupled plasmon-phonon modes and so the oscillations observed cannot be assigned to those collective modes.[3–5] It is important that the frequencies of oscillations remain unchanged by varying laser power in the range of 6–16 mW (the electron density photoexcited $n_q=1.1\times 10^{19}-3.4\times 10^{19}\ \mathrm{cm}^{-3}$, respectively). This is demonstrated for the thinner LT-GaAs slab PS in Fig. 3 (inset). The plasma frequency for the mentioned carrier densities photoexcited in LT-GaAs can be estimated to be in the range $\omega_p=6.3-11.2$ THz, respectively. Here we used the following parameters for LT-GaAs: $\varepsilon_0\varepsilon=1.14\times 10^{-10}$ F/m and $m^*=0.067m_0$, where m_0 is the free electron mass. The latter fact suggests again that the THz oscillations observed cannot be assigned to the regular plasma oscillations, at which the carriers coherently oscillate at the plasma frequency.[1,2] Also, it should be noted that the oscillations discussed have nothing to do with the Gunn effect because of the much higher frequency range.[8,9] Thus, we believe that the observed oscillations result from plasma waves generated in LT-GaAs under special conditions involving the thickness of the μm-sized LT-GaAs slab as a parameter. Specifically, we believe that THz oscillations manifest themselves as a consequence of the standing plasma waves created in the LT-GaAs slab, which acts as a resonant cavity. The standing waves are created due to the successive reflections of traveling plasma

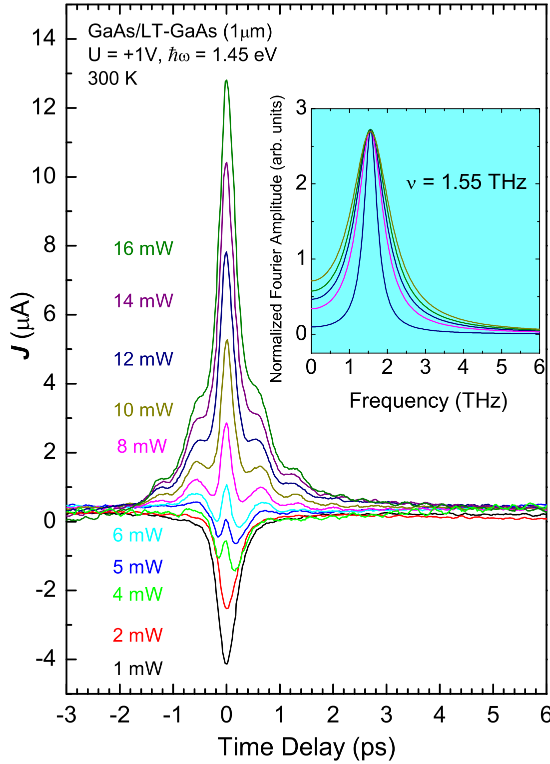

FIG. 3. (Color online) The photocurrent autocorrelation signals from the GaAs/LT-GaAs PS with 1-μm thick LT-GaAs slab measured with photon energy 1.45 eV as a function of the laser power indicated. The inset shows by the corresponding colors the result of the Fourier transformation of the oscillatory part of the signals.

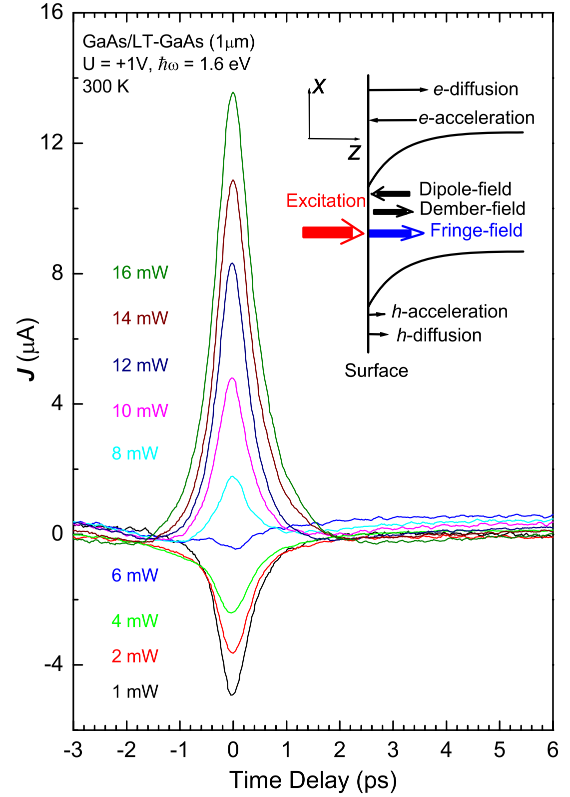

FIG. 4. (Color online) The photocurrent autocorrelation signals from the GaAs/LT-GaAs PS with 1-μm thick LT-GaAs slab measured with photon energy 1.6 eV as a function of the laser power indicated. The inset shows schematically the directions of the fringe and light-induced transient fields.

waves from the LT-GaAs slab boundaries. Because the frequency of standing plasma waves generated is much less than ω_p, the microscopic picture of the THz oscillation observed can be imagined as a modulation of the high-frequency plasma oscillations by the lower frequency plasma wave. The frequency of THz oscillations hence does not depend on the carrier density photogenerated in the slab (Fig. 3) and is exclusively determined by the resonant cavity parameters (the LT-GaAs slab thickness). The remarkable feature manifests itself in the power dependence of the photocurrent signal measured within the range of the laser power of 1–16 mW (the electron density photoexcited $n_q \sim 2.1 \times 10^{18} - 3.4 \times 10^{19}$ cm^{-3}, respectively). Figure 3 shows the effect of the laser power increase on the photocurrent signal, which reveals the dynamics of the generation of THz oscillations including a threshold feature. The thresholdlike behavior for the resonant plasma wave generation has been predicted for GaAs-based HEMT (Refs. 10–12) and evidenced experimentally for voltage tunable resonant THz emission.[13]

Let us consider the origin of the plasma wave generation in the LT-GaAs slab. As we mentioned above the photocurrent in the PS arises as a consequence of the carrier density photoexcited in the PS material. As this takes place, the electrons carry the main part of the photocurrent flowing between the PS contacts along the surface (x axis). Since the carriers are photoexcited in the presence of bias electric field, the z-component of the field (the fringe field) tends the electrons to be accelerated toward the material surface.[16–18] The photoexcited holes hence are accelerated in the opposite direction. As a result, a dipole field is formed, which is directed against the fringe field (Fig. 4 inset). On the other hand, the carrier density photoexcited in the material is characterized by the Beer's law distribution and hence the density gradient drives diffusion of electrons and holes into the material from the surface, i.e., in a direction perpendicular to the surface (z axis). Because the mobility of the electrons is higher than that of the holes the photo-Dember field arises,[16–18] which is directed along the fringe field (Fig. 4 inset). Thus, additionally to the photocurrent flowing between PS contacts, the femtosecond laser pulse generates the transient electrical currents in z direction associated with carrier drift (J_E) and carrier diffusion (J_D) (Refs. 16–18):

$$J_z(t) = J_E(t) + J_D(t) = q(n_q\mu_q + n_p\mu_p)\,\nabla\,\phi - q(D_q\,\nabla\,n_q - D_p\,\nabla\,n_p), \qquad (1)$$

where n_q and n_p denote the density of electrons and holes, $\mu_q \gg \mu_p$ are the electron and hole effective mobility, ϕ is the electric potential in the surface field region, and $D_q = \mu_q k_B T_q / q$ and $D_p = \mu_p k_B T_p / q$ are the corresponding carrier diffusion coefficients. The sign "–" in Eq. (1) between two terms describing the carrier drift and the carrier diffusion

distinguishes the opposite direction of the transient electrical current flow mentioned above.

The dynamics shown in Fig. 3 clearly demonstrates that the photocurrent direction in the PS can be reversed by increasing the carrier density photoexcited in the sample. Moreover, there exists some critical carrier density, at which the photocurrent is nearly not flowing despite the constant electrical bias applied. To discuss this peculiarity we consider a simple current shunt model, which takes into account that the total current flowing between PS contacts is determined by a sum of two currents. One of them is the current flowing in x direction exactly in the near-surface region. This current includes both the dark current $J_{dx}(t)$ and the photocurrent $J_{px}(t)$. Another portion of the total current is the shunt current, which flows in the deeper region of the material and so includes a significant z component $[J_z(t)]$. Thus, the total current flowing through the PS strongly depends on the z component of the current. Because the main dynamical changes in the electron density photoexcited occur along z direction, the photocurrent autocorrelation response is mainly caused by the z component of the photocurrent. Alternatively, the x component of the photocurrent only sets up a background of the signal, which is close to the zero level since the x component of the photocurrent is expected to be much weaker than the z component.

We associate the dynamics shown in Fig. 3 with competition between two contributions into the total current flowing through the PS. It is clear from Eq. (1) that both the drift-related and diffusion-related transient electrical currents flowing in z direction depend on the carrier density photoexcited in the material. Here we took into account that $n_q/\nabla n_q = n_p/\nabla n_p = L$ is the absorption length. However, the diffusion-related transient electrical current is expected to be dominant with increasing carrier density (with increasing laser power). This is because the mobile carriers photoexcited in the material screen the fringe field and so decrease the drift-related current with increasing carrier density. Hence, the first contribution into the photocurrent which appears at low carrier densities is caused by the drift-related current. The corresponding photocurrent autocorrelation signal is negative.[15] The second contribution which becomes dominant with increasing carrier density is related to the diffusion of carriers due to the density gradient (Fig. 4 inset). This contribution gives rise to a positive signal. Thus, the signal sign reverse feature shown in Fig. 3 results from the competition between the carrier drift and carrier diffusion processes occurring in the photoexcited electron-hole plasma. An increase in the carrier density up to the threshold value of $\sim 1.1\times 10^{19}$ cm^{-3} leads to the plasma waves to be generated in the plasma. It is evident now that the plasma waves arise as a consequence of the instantaneous diffusion of photoexcited carriers inward the PS material and their shock interaction with the GaAs/LT-GaAs interface. The reverse of the sign of the photocurrent autocorrelation signals with carrier density also suggests that the generation mechanism of THz oscillations is related to the transient current flow and so excludes from consideration the optical rectification effect.[19] The diffusion-induced dynamical variation of the density of the Beer's law distributed electrons at the GaAs/LT-GaAs interface leads to the dynamical electric field to be formed, which can be monitored through the TRC responses by measuring them simultaneously with photocurrent. As we will show below, such an experimental approach unambiguously proves that the plasma wave generation process is related to the instantaneous carrier diffusion. The reflection of plasma wave from the LT-GaAs slab borders leads to the standing wave with zero group velocity in the LT-GaAs slab to be formed. The frequency of oscillations can hence be tuned in the THz range by the thickness of the slab. The electrostatic field of the plasma standing wave periodically modulates the photoexcited plasma within the LT-GaAs slab and so additionally affects the fringe field in the material. As a result, the electron plasma standing waves give rise to the photocurrent autocorrelation signals. The frequency of oscillations hence is determined by the number of antinodes in the standing plasma wave formed in the slab. Such a behavior of a plasma slab of finite width due to localized electrostatic perturbations is well known in plasma physics, which takes into account the localized plasma waves and a standing-wave electrostatic field.[20]

Taking into account that the typical electron thermal velocity in GaAs is of $v_{\mathrm{th}} = 4.4\times 10^5$ m/s, one can estimate the inverse electron transit time (v_{th}/d, where d is the thickness of the slab) in LT-GaAs as 0.44 and 0.22 THz for 1-μm and 2-μm thick LT-GaAs slab samples, respectively. The frequencies of THz oscillations observed are $\sim$3.5 times larger than the values obtained. This is a reason why the oscillations observed are not associated with the carrier transport despite the fact that their generation mechanism involves the instantaneous diffusion of carriers driven by the photoexcited carrier density gradient. The plasma waves propagate in the "ballistic" regime. This is because the laser photon energy used is just 20 meV higher than the bandgap of GaAs ($E_g = 1.43$ eV). The relaxation of nonequilibrium (hot) electrons in LT-GaAs is known to be due to the electron-LO-phonon scattering and trapping by As cluster point defects.[21] However, since the energy of photoexcited nonequilibrium electrons in the conduction band of LT-GaAs is less than the 36 meV LO phonon energy, the electron-phonon relaxation is highly improbable. As a result, the ultrafast electron dynamics under the excitation regime used is exclusively determined by the electron-electron thermalization and electron trapping processes. It is evident that the "ballistic" regime for plasma wave propagation can be achieved when the plasma wave period is less than the lifetime of free carriers in LT-GaAs, which lies in the subpicosecond range due to all of the traps.[21] The plasma waves generated die out with increasing photon energy, indicating that the electron-LO-phonon scattering damps the "ballistic" regime of plasma wave propagation. This is demonstrated in Fig. 4 with photocurrent autocorrelation signals measured in the same range of the laser powers but with photon energy 1.6 eV.

As we mentioned above, the THz oscillations observed are due to the standing plasma waves generated in the resonant cavity, which is formed by LT-GaAs slab borders. Let us consider now why such waves appear in the photocurrent autocorrelation measurements. In general terms, the photocurrent generated by two laser beams is an averaging over the laser pulse repetition frequency $(1/T)$ (Refs. 14 and 15):

$$J(\tau) \propto \frac{1}{T}\int_{-\infty}^{+\infty}[n_q(t)+n_q(t+\tau)]dt, \quad (2)$$

where τ is the relative time delay between two laser pulses. It should be noted that the model which has been used in Refs. 14 and 15 to analyze the photocurrent response induced by two laser beams was based on an assumption that the output signal depends only upon the instantaneous number of photogenerated carriers n_q and all the effects related to carrier drift and diffusion have been ignored. In contrast, in our consideration here the mentioned effects cause the primary source of the plasma wave generation and in turn drive the THz oscillations observed. Because the autocorrelation of electric fields photogenerated in the material by two laser beams is determined by the degree of coherence of fields, one should distinguish between the coherent and incoherent part of the measured signal. As a result, the photocurrent generated in the PS consists of two contributions: the autocorrelation and "memory" effects $[J(\tau)=J_{AC}(\tau)+J_M(\tau)]$. The first of them is a coherent response, which is due to the nonlinear dependence of the carrier photogeneration rate on the laser light intensity. The nonlinearity of the primary photogeneration process is not conclusively established but it is believed to be attributed to the two-photon absorption, free carrier absorption, Auger heating, or impact ionization. The photocurrent autocorrelation response is hence expected to be due to the nonthermalized electron density autocorrelation. Remember here that the term "thermalization" is applied to characterize the electron-electron thermalization process while the term "nonequilibrium" points to the electron-LO-phonon scattering and electron trapping processes. Since the electron-electron thermalization time (τ_t) for the carrier density of 7.0×10^{18} cm^{-3} has been measured to be $\sim$14 fs,[22] the nonthermalized electron density autocorrelation signal,[14,15]

$$J_{AC}(\tau) \propto \frac{1}{T}\int_{-\infty}^{+\infty}[n_q(t)n_q(t+\tau)]dt, \quad (3)$$

is just slightly broader than the laser light autocorrelation pulse (Fig. 2). The primary nonlinearity of the photogeneration rate persists for plasma waves generated by each of the laser pulses as well, giving rise to the corresponding coherent contribution into the photocurrent signal $[J_{AC}^W(\tau)]$. As a result, the electron density autocorrelation occurs as a consequence of the interaction between plasma waves, which can be described by damped exponential cosine functions. The resulting photocurrent autocorrelation response is given as follows:

$$J_{AC}^W(\tau) \propto \frac{1}{T}\int_{-\tau_{DT}/2}^{\tau_{DT}/2}\cos(2\pi\nu t)\cos[2\pi\nu(t+\tau)]e^{-(2t+\tau)/\tau_{DT}}dt, \quad (4)$$

where ν is the frequency of oscillations, and τ_{DT} denotes the plasma wave damping time in LT-GaAs. The incoherent response (the "memory" effect) just points to the dependence of the electron photogeneration rate for delayed pulse on the density of carriers that already exist in the sample due to the action of the initial pulse and lost their coherence. This is a reason why such a photoexcitation regime is called a "memory" effect. Actually the "memory" effect is believed to have the same nature as the well known phase space filling effect (the absorption bleaching) in pump-probe optical spectroscopy; hence, the term "memory effect" is used just to distinguish it from that in optical measurements. Accordingly, the absorption coefficient in the absorption bleaching effect is given by $\alpha=\alpha_0(1-f_e-f_h)$, where f_e and f_h are the Fermi–Dirac occupancy factors for electrons and holes, respectively, and α_0 is the absorption coefficient with no pump applied.[23] Because the incident laser light initially sets up an exponentially decaying distribution of photoexcited carriers along the direction z in accordance with Beer's absorption law: $n_q(z,t)=n_{q0}\exp(-\alpha z)$, where n_{q0} is the carrier density photoexcited at the sample surface, the absorption length in the PS material for the delayed pulse becomes longer and at the same time the carrier photogeneration rate decreases during the lifetime of carriers photoexcited by the initial pulse. Thus, the "memory" effect actually describes the lifetime of nonequilibrium carriers in LT-GaAs (Ref. 15):

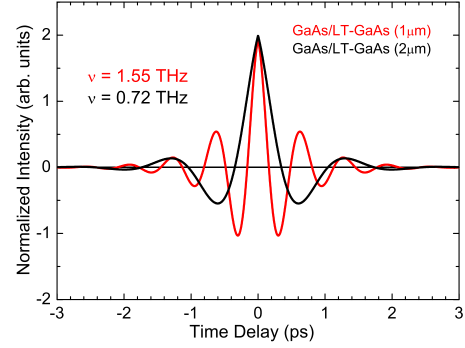

FIG. 5. (Color online) The oscillatory part of the photocurrent signals from the GaAs/LT-GaAs PS's of different thicknesses of the LT-GaAs slab (shown by the corresponding colors).

$$J_M(\tau) \propto \frac{1}{T}e^{-|\tau/\tau_{D1}|}. \quad (5)$$

Integrating Eq. (4) over the plasma wave damping time and taking into account that the second-order autocorrelation function can analytically be presented in sech^2 form, one can get the final expression for the photocurrent response:

$$J(\tau) = a_1\,\mathrm{sech}^2\left(\frac{K\tau}{\tau_t-\tau_0}\right) + a_2[\cos(2\pi\nu\tau)]e^{-|\tau/\tau_{DT}|} + a_3 e^{-|\tau/\tau_{D1}|}, \quad (6)$$

where a_1, a_2, and a_3 are coefficients, $\tau_0=0.15$ ps is the laser light pulse width, and $K=1.54$ is a coefficient, which sets up a correspondence between the real pulse width and the sech^2 function width. The result of the fit by Eq. (6) to the data measured is shown in Fig. 2. The oscillatory part of the signals extracted from the fit curves is shown in Fig. 5. The result of the fit shows that the few-cycle THz oscillations damp fast enough with a constant of $\tau_{DT}=0.45$ ps, which is similar to τ_{D1} denoting a typical lifetime of free electrons in LT-GaAs materials.[21] From this we conclude that the Landau

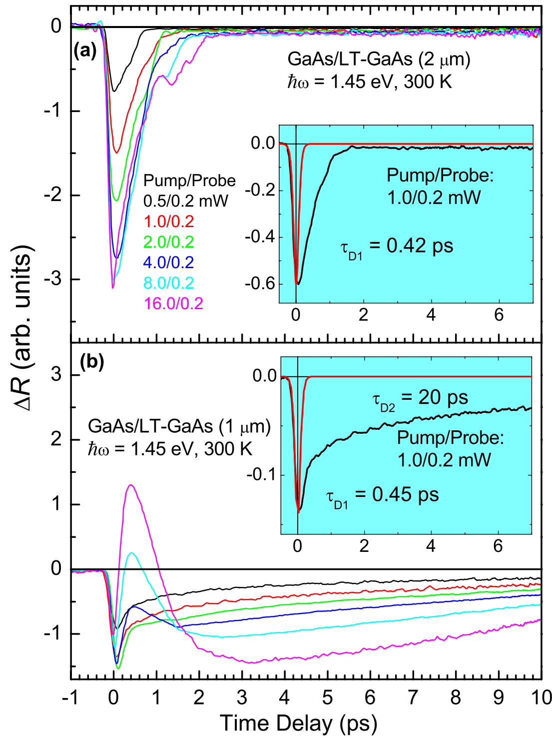

FIG. 6. (Color online) The TRC signals from GaAs/LT-GaAs PS's of different thicknesses of the LT-GaAs slab [2 μm (a) and 1 μm (b)] measured as a function of the pump beam power indicated by the corresponding colors. The insets show one of the TRC signals (shown in black) and the laser light autocorrelated pulse (shown in red).

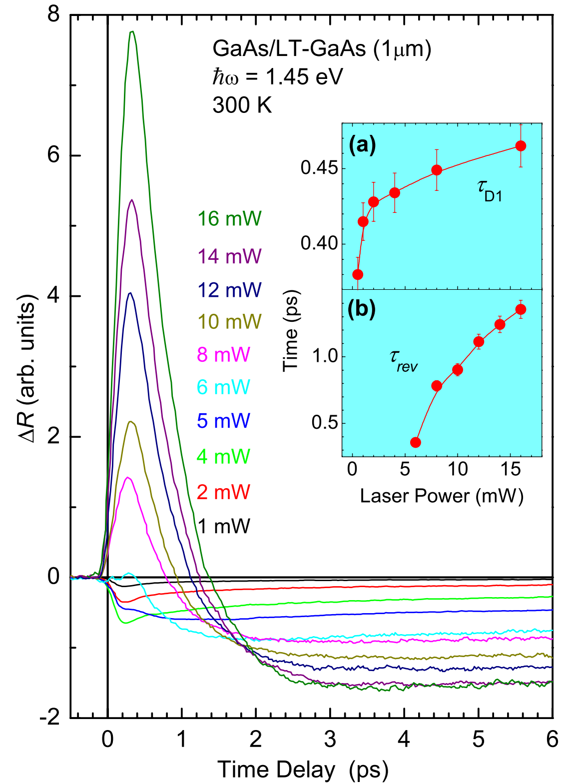

FIG. 7. (Color online) The TRC signals from the GaAs/LT-GaAs sample of 1-μm thick LT-GaAs slab measured as a function of the laser power indicated by the corresponding colors. The inset shows the pump beam power dependence of the decay-time constant τ_{D1} measured for 2-μm thick LT-GaAs slab and t_{rev} measured for 1-μm thick LT-GaAs slab.

damping of localized plasma waves (transit-time damping)[20] is inefficient for plasma waves generated in the system under consideration.

The velocity of plasma waves propagating in the LT-GaAs slab and reflecting from its boundaries is given by: $s = 2\nu d/N$, where an integer $N=1,2,3,\ldots$ is the number of antinodes in the standing plasma wave. Figure 5 shows that $N=3$. One can get the following values of velocities for plasma waves: $s \sim 1.03\times10^6$ m/s and $\sim 0.96\times10^6$ m/s for the samples of 1-μm and 2-μm thick LT-GaAs slab, respectively. The plasma wave velocities obtained are close to the typical ballistic electron velocity of $\sim 0.8\times10^6 - 0.9\times10^6$ m/s estimated for GaAs-based devices.[24]

B. Transient reflectivity change responses and the dynamical electric field at the GaAs/ low-temperature-grown-GaAs interface

Now we need to focus on the nature of the dynamical electric field at the GaAs/LT-GaAs interface. This field can be monitored through the TRC signals, which have been measured simultaneously with photocurrent. First we consider the pump beam power dependence of the TRC signals measured in a typical pump-probe configuration when the power of the probe beam was unchanged and set up to be much smaller than the power of the pump beam (Fig. 6). The TRC signal from the 2-μm thick LT-GaAs slab sample shows a typical negative feature, the amplitude of which increases with pump power [Fig. 6(a)]. The signal is associated with the phase space filling effect (the absorption bleaching).[23,25] The rise-time of the signal is due to the electron-electron thermalization process. An increase in the pump power within the range of 0.5–16 mW (the electron density photoexcited $n_q \sim 1.1\times10^{18} - 3.4\times10^{19}$ cm^{-3}, respectively) does not affect the rise-time of the TRC signals, indicating the temporal resolution limit. Since the rise of the signal closely matches the laser pulse-front [Fig. 6(a) inset], one can estimate the rise-time constant to be ≤ 10 fs. As we mentioned above, this time is consistent with 14 fs electron-electron thermalization time measured at the carrier density of 7.0×10^{18} cm^{-3}.[22] The signal decays with a constant of τ_{D1}, which lies in the subpicosecond range and varies with pump power as shown in Fig. 7 [inset (a)]. The values obtained agree well with the known lifetime of free electrons in LT-GaAs materials.[21]

The TRC signals from the 1-μm thick LT-GaAs slab sample reveal an additional much longer decay-time component (τ_{D2}), which we associate with the lifetime of free electrons in the GaAs substrate [Fig. 6(b)]. We note here that the experimental setup used in our measurements was incapable of measuring long decay times. Therefore, the decay-time constants mentioned in the current paper for GaAs just argue that the lifetime of free carriers in the GaAs substrate is much longer than that in LT-GaAs. The TRC signals tend to

show a positive contribution with increasing pump power, which manifests itself additionally to the absorption bleaching component. Such a positive contribution can also be recognized with much smaller amplitude for the 2-μm thick LT-GaAs slab sample if the maximal pump power is applied [Fig. 6(a)]. We associate the positive contribution into the TRC signal with that induced through the electro-optic effect by the dynamical electric field at the GaAs/LT-GaAs interface. As a result, the experimental data shown in Fig. 6(b) suggest that there is a dynamical reverse of the electric field with increasing carrier density photoexcited. The existence of the dynamical electric field which is localized at the GaAs/LT-GaAs interface and dominantly contribute into the TRC signals at high electron densities explains why the applied bias field does not affect the TRC signals.

Now let us consider the TRC responses measured simultaneously with the photocurrent signals when the power of both beams has been set up to be equal (compare the corresponding curves in Figs. 3 and 7). It is of first importance that the positive component of the TRC signal due to the electro-optic contribution becomes dominant at the same laser powers at which the THz oscillations in the photocurrent signals begin to appear. From this we conclude that the plasma waves are generated at a certain carrier density photoexcited, at which the instantaneous diffusion of carriers inward the material is able to modify the initially Beer's law distributed carrier density at the GaAs/LT-GaAs interface, forming an electric field at it. The resulting dynamical electric field contributes into the TRC signals though the electro-optic effect.

According to Fresnel equations, the reflection coefficient at normal incidence is given by: $R=(1-n)^2/(1+n)^2$. One can show that the TRC is[25]

$$\Delta R(t) = 4(n^2-1)\Delta n(t)/(n+1)^4 = 2(\delta-1)\Delta\delta(t)/\delta^{1/2}(\delta^{1/2}+1)^4, \quad (7)$$

where $\Delta n \ll n$ is a change in the refractive index (n) and correspondingly $\delta=\varepsilon^{-1}$ is the inverse of the dielectric tensor ($\varepsilon=n^2$). For anisotropic media the linear and quadratic electro-optic coefficients (r_{ijz} and p_{ijzz}, respectively) can be defined as follows:[26]

$$\Delta\delta_{ij}(t) = r_{ijz}E_{0z}(t,z) + p_{ijzz}E_{0z}(t,z,)E_{0z}(z,t) + \ \ldots \ . \quad (8)$$

Here we assume that an effective interfacial electric field $[E_{0z}(t,z)]$ due to the electron density variation at the GaAs/LT-GaAs interface is directed along the z axis. As we mentioned above, the population of photoexcited carriers will exist in the GaAs substrate as well as the LT-GaAs slab. The instantaneous density of spatiotemporally distributed electrons photoexcited in GaAs/LT-GaAs sample is given as follows:

$$n_q(t,z) = n_{q0}(1-e^{-t/\tau_t})e^{-t/\tau_D}e^{-\alpha z}, \quad (9)$$

where τ_t and τ_D are the rise-time and decay-time constants associated with the electron-electron thermalization and electron trapping processes, respectively. As it has been discussed above, due to the density gradient within the Beer's law distributed electron population, the electron diffusion inward the sample occurs. Since the density gradient region is extended over the entire thickness of the LT-GaAs slab as well as the part of the GaAs substrate, the electron density in the LT-GaAs slab nearby the GaAs/LT-GaAs interface rises up owing to the limited electron diffusion across it. Alternatively, the electron density in the GaAs substrate in the vicinity of the GaAs/LT-GaAs interface is reduced due to the carrier diffusion into the substrate. The strength of the electric field at the interface hence is expected to be proportional to the difference of electron densities delivered to the interface within the LT-GaAs slab and that rejected from the interface into the GaAs substrate during an effective time τ_w which is associated with electron diffusion and is assumed to be $\tau_w \gg \tau_t$ [Fig. 1(c)]. Hence, taking into account the distribution in the form of Eq. (9), the strength of the interfacial electric field can be written in the following form:

$$E_{0z}(t) \propto \frac{q}{\varepsilon_0\varepsilon}(1-e^{-t/\tau_w})\left[\int_0^d n_{q1}(t,z)dz - \int_d^L n_{q2}(t,z)dz\right] = \frac{qn_{q0}}{\alpha\varepsilon_0\varepsilon}(1-e^{-t/\tau_w})[(1-e^{-\alpha d})e^{-t/\tau_{D1}} - e^{-\alpha d}(e^{-\alpha L}-e^{-\alpha d})e^{-t/\tau_{D2}}], \quad (10)$$

where n_{q1} and n_{q2} are the densities of photoexcited carriers in the LT-GaAs slab and the GaAs substrate, respectively; d and L denote the thickness of the LT-GaAs slab and the light penetration depth (absorption length) in the samples. Because the electron lifetime in LT-GaAs is much shorter than that in GaAs, the electric field at the interface is reversed at some characteristic time, $t_{\mathrm{rev}}(E_{0z}=0)$ [Fig. 1(c)], which is determined by the thickness of the LT-GaAs slab and the material parameters:

$$t_{\mathrm{rev}} = \frac{\tau_{D1}\tau_{D2}}{\tau_{D2}-\tau_{D1}}\ln\left[\frac{(1-e^{-\alpha d})}{e^{-\alpha d}(e^{-\alpha L}-e^{-\alpha d})}\right]. \quad (11)$$

Thus, the electric field at the GaAs/LT-GaAs interface initially rises up with a constant of τ_w and then falls down reversing at t_{rev}. Such a behavior is due to the dynamical variation in the density of the Beer's law distributed electrons at the GaAs/LT-GaAs interface involving both the hampered diffusion of carriers across the GaAs/LT-GaAs interface and the difference in the free carrier lifetimes for GaAs and LT-GaAs materials. This is a reason why the electric field at the GaAs/LT-GaAs interface can be called a dynamical electric field. Figure 7 clearly demonstrates that t_{rev} becomes longer with increasing carrier density. This is consistent with Eq. (11) since $\tau_{D2} \gg \tau_{D1}$ and τ_{D1} increases with laser power (Fig. 7 insets). It is evident that the strength of the dynamical electric field has to be much lower for the thicker LT-GaAs slab sample because, as we mentioned above, the smaller carrier population is photoexcited in the GaAs substrate for that PS. This correlates also with the smaller amplitude of THz oscillations observed in the photocurrent autocorrelation responses from thicker LT-GaAs slab PS. The latter fact indicates that the amplitude of THz oscillations observed is determined by the density of carriers in the vicinity of the GaAs/LT-GaAs interface, which exponentially decays for thicker LT-GaAs slabs in accordance with

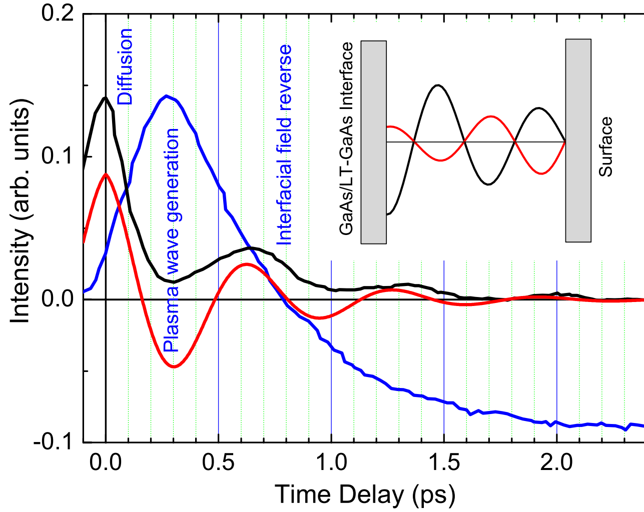

FIG. 8. (Color online) The arbitrary normalized photocurrent autocorrelation and TRC signals (in black and blue, respectively) from the GaAs/LT-GaAs PS of 1-μm thick LT-GaAs slab measured simultaneously with pump and probe beams powers of 8 mW. The oscillatory part of the photocurrent autocorrelation signal extracted from the fit is shown in red. The inset shows the sketch of the partially standing wave in the photoexcited electron plasma.

Beer's absorption law. According to Eqs. (7) and (8), the dynamical electric field at the GaAs/LT-GaAs interface contributes to the TRC signals through the electro-optic effect.[25] Correspondingly, the TRC signals reveal the positive contribution, which increases with the density of photoexcited carriers (with an increase in the laser power) and becomes dominant for thinner LT-GaAs slab samples (Figs. 6 and 7).

The TRC signals for which the electro-optic contribution becomes dominant can be fitted by Eq. (10). Figure 2(b) (inset) shows an example of the fit. The fit gives the following parameters: τ_w=0.18 ps, τ_{D1}=0.43 ps, $t_{\rm rev}$=0.83 ps, and τ_{D2}=38 ps. The effective time τ_w, which is associated with electron diffusion, is just slightly longer than the laser pulse width. This suggests that the instantaneous diffusion of photoexcited carriers leads to a shock interaction of carriers with the GaAs/LT-GaAs interface. As we mentioned above, such a feature is considered as the origin for the plasma waves to be generated toward the surface. Since the dynamical electric field is reversed at $t_{\rm rev}$=0.83 ps while the plasma wave damps with a constant τ_{DT}=0.45 ps, the electric field reverse at the GaAs/LT-GaAs interface does not strongly affect the plasma wave dynamics. The electro-optic contribution remains weak enough for the thicker LT-GaAs slab sample [Fig. 2(a) inset], indicating that a much weaker dynamical electric field at the interface is created.

Figure 8 summarizes the experimental findings discussed in the current paper. One can see from the TRC response that the dynamical electric field due to the carrier diffusion toward the PS material rises up with a constant of τ_w =0.18 ps, which is comparable to the laser pulse width. This leads to the shock interaction of the photoexcited electron plasma with the GaAs/LT-GaAs interface and in turn to the generation of plasma wave in the time frame of 0.2–0.3 ps. The plasma wave travels toward the surface and reflects from it. The resulting standing plasma wave is formed as a consequence of interaction of initially generated and reflected traveling waves. Because of the finite lifetime of free carriers in the LT-GaAs slab, the plasma wave quickly damps. As a result, the condition for the standing plasma wave formation is mostly fulfilled only for the nearest to the surface antinode. Such a partially standing plasma wave forms the periodic axial wakefields over the slab, the amplitude of which hence decreases inward the material. Since the wakefields affect the bias fringe field in the vicinity of the surface, the spatial modulation of the photoexcited plasma appears in the photocurrent autocorrelation signals. For the same reason the wakefields do not affect the electric field at the GaAs/LT-GaAs interface and hence the corresponding TRC signals measured simultaneously with photocurrent do not reveal any oscillation.

IV. CONCLUSIONS

In summary, we have provided experimental evidence that the THz oscillations can be generated by a femtosecond optical pulse in the μm-sized LT-GaAs slab grown on the GaAs substrate. The frequency of oscillations is inversely proportional to the thickness of the LT-GaAs slab. The oscillations have been measured by using the photocurrent autocorrelation technique and appear due to the spatial modulation of photoexcited plasma by the standing plasma wave created as a consequence of the interaction of traveling plasma waves in the resonant cavity formed by the LT-GaAs slab boundaries. The transient reflectivity change responses which have been measured simultaneously with photocurrent autocorrelation signals reveal the mechanism of plasma wave generation. It has been shown that the initial instantaneous diffusion of photoexcited carriers driven by the density gradient over the Beer's law distributed carrier population is the main reason for the shock interaction of the photoexcited plasma with the GaAs/LT-GaAs interface, which results in the generation of plasma waves. The standing plasma waves created in the LT-GaAs slab behave similarly to the standing optical waves in the Fabry–Perot resonant cavity and so their frequency can be tuned in the THz range by the thickness of the LT-GaAs slab.

ACKNOWLEDGMENTS

This research was supported by the German Science Foundation. Y.D.G. gratefully acknowledges support from the Max-Planck Society.

*Corresponding author. Present address: U.S. Army Aviation and Missile RDEC, Redstone Arsenal, AL 35809, USA.
†Nano and Micro Devices Center, University of Alabama in Huntsville, AL 35899, USA; glinkay@uah.edu

[1] W. Sha, A. L. Smirl, and W. F. Tseng, Phys. Rev. Lett. **74**, 4273 (1995).
[2] R. Kersting, K. Unterrainer, G. Strasser, H. F. Kauffmann, and E. Gornik, Phys. Rev. Lett. **79**, 3038 (1997).
[3] G. C. Cho, W. Kütt, and H. Kurz, Phys. Rev. Lett. **65**, 764 (1990).
[4] Y. M. Chang, L. Xu, and H. W. K. Tom, Phys. Rev. Lett. **78**, 4649 (1997).
[5] G. C. Cho, T. Dekorsy, H. J. Bakker, R. Hövel, and H. Kurz, Phys. Rev. Lett. **77**, 4062 (1996).
[6] B. B. Hu, A. S. Weling, D. H. Auston, A. V. Kuznetsov, and C. J. Stanton, Phys. Rev. B **49**, 2234 (1994).
[7] A. V. Kuznetsov and C. J. Stanton, Phys. Rev. B **48**, 10828 (1993).
[8] J. B. Gunn, Solid State Commun. **1**, 88 (1963).
[9] W. Knap, Y. Deng, S. Rumyantsev, and M. S. Shur, Appl. Phys. Lett. **81**, 4637 (2002).
[10] M. I. Dyakonov and M. S. Shur, IEEE Trans. Electron Devices **43**, 380 (1996).
[11] M. I. Dyakonov and M. S. Shur, Phys. Rev. Lett. **71**, 2465 (1993).
[12] M. Dyakonov and M. S. Shur, in *Terahertz Sources and Systems*, edited by R. E. Miles (Kluwer, Netherlands, 2001), pp. 187–207.
[13] W. Knap, J. Lusakowski, T. Parenty, S. Bollaert, A. Cappy, V. V. Popov, and M. S. Shur, Appl. Phys. Lett. **84**, 2331 (2004).
[14] T. F. Carruthers and J. F. Weller, Appl. Phys. Lett. **48**, 460 (1986).
[15] M. Griebel, J. H. Smet, D. C. Driscoll, J. Kuhl, C. A. Diez, N. Freytag, C. Kadow, A. C. Gossard, and K. von Klitzing, Nat. Mater. **2**, 122 (2003).
[16] A. Leitenstorfer, S. Hunsche, J. Shah, M. C. Nuss, and W. H. Knox, Phys. Rev. Lett. **82**, 5140 (1999).
[17] J. N. Heyman, N. Coates, A. Reinhardt, and G. Strasser, Appl. Phys. Lett. **83**, 5476 (2003).
[18] M. Nakajima, M. Hangyo, M. Ohta, and H. Miyazaki, Phys. Rev. B **67**, 195308 (2003).
[19] S. L. Chuang, S. Schmitt-Rink, B. I. Greene, P. N. Saeta, and A. F. J. Levi, Phys. Rev. Lett. **68**, 102 (1992).
[20] R. W. Short and A. Simon, Phys. Plasmas **5**, 4124 (1998).
[21] G. Segschneider, T. Dekorsy, H. Kurz, R. Hey, and K. Ploog, Appl. Phys. Lett. **71**, 2779 (1997).
[22] P. C. Becker, H. L. Fragnito, C. H. Brito Cruz, R. L. Fork, J. E. Cunningham, J. E. Henry, and C. V. Shank, Phys. Rev. Lett. **61**, 1647 (1988).
[23] W. H. Knox, C. Hirlimann, D. A. B. Miller, J. Shah, D. S. Chemla, and C. V. Shank, Phys. Rev. Lett. **56**, 1191 (1986).
[24] L.-E. Wernersson, A. Litwin, L. Samuelson, and H. Xu, Mater. Sci. Eng., B **51**, 76 (1998).
[25] Y. D. Glinka, N. H. Tolk, X. Liu, Y. Sasaki, and J. K. Furdyna, J. Appl. Phys. **103**, 043708 (2008).
[26] Y. R. Shen, *Principles of Nonlinear Optics* (Wiley, New York, 1984).